Applicability of Linear Elastic Fracture Mechanics to 5.6-mil Boron/6061 Aluminum

J. P. Waszczak*
General Dynamics Convair Division, San Diego, Calif.

A coordinated experimental and analytical program was directed toward assessing the applicability of linear elastic fracture mechanics to 5.6-mil boron/6061 aluminum subjected to Mode I loading. Fifty-nine standard ASTM three-point bend and center-notched specimens were tested. The effects of laminate orientation, specimen thickness, crack length, specimen configuration, and heat treat condition on laminate fracture toughness are reported. A technique of predicting the fracture toughness of an arbitrary $(0/\pm a/90)$ laminate from critical strain energy release rate data for 0-, $\pm a$-, and 90° specimens was evaluated for $(0/\pm 45)$ boron/aluminum.

Introduction

In the past few years a number of investigators have applied linear elastic fracture mechanics (LEFM) successfully to several resin-matrix composite material systems.[1,2] Now that metal-matrix composite materials have become cost competitive, it is necessary to determine whether LEFM is applicable to metal-matrix composite systems.

Physical observations regarding the failure mechanism exhibited by boron/aluminum (B/Al) have recently been made that support the idea that fracture mechanics is required to predict the static strengths of flawed (machined or damaged) B/Al specimens. The first observation involved visual slow crack growth emanating from a circular hole in $(0/\pm 45)_s$ boron/aluminum. This phenomenon occurs in tensile coupons containing circular holes and single-fastener bolt bearing specimens, for both heat-treated and the as-received (condition F) boron/aluminum. Typical damage is shown in Fig. 1 for these two specimen geometries. This physical evidence also supports the inherent flaw concept discussed in Ref. 2. A second source of supporting data involved impact damage on a unidirectional (UD) B/Al tube. Figure 2 shows an x-ray of a four-ply tube, which had been impacted using a blunt penetrator. The penetrator had a tip radius of curvature of 2 in., weighed approximately 4 lb, and was dropped from 20 ft. As is clear in Fig. 2, the damage at the impact location took the form of a through crack extending across approximately 15 fiber diameters. Although a static test of this tube has yet to be performed, a fracture mechanics analysis will be used to predict the ultimate load. The third visual observation of physical cracks involved failed static unidirectional unflawed tensile coupons. Several such tension specimens in which damage was observed at locations away from the failure initiation point, similar to that shown in Fig. 3, have been tested at Convair. Here, a series of broken fibers was generated during the tension loading of a four-ply coupon. It is believed that similar damage slowly accumulated at the actual failure location and became critical before the damage shown in Fig. 3 could become critical. It has been observed in B/Al-to-titanium joints that continuous fibers adjacent to a terminated ply often are broken during fabrication in bending, as illustrated in Fig. 4. This type of damage can be represented by a part-through crack in the boron/aluminum. In all four of the above cases, the physical damage indicates that a fracture model would be appropriate for determining static strengths of these test specimens.

The coordinated experimental and analytical program reported herein assesses the applicability of LEFM to 5.6-mil boron/6061 aluminum, both condition F (as received) and STCA (solution treated, cryogenically quenched and aged). The results of this study will be used in the future to predict residual strengths for various flawed B/Al structures, including structures that have been damaged through impact-type loadings.

Background

All resin-matrix and metal-matrix composite material systems exhibit some degree of nonlinear behavior. In both cases the matrix material controls the degree of nonlinearity in laminate response. The overall laminate response of a fiber-dominated resin-matrix laminate is quite linear, since the ratio of fiber to matrix stiffness is about 80 to 1 for graphite/epoxy (G/E) and 120 to 1 for boron-epoxy (B/E).[3] In the case of B/Al, however, this ratio is only about 6 to 1, which means a $(0/\pm\alpha)$ B/Al laminate can behave in a very nonlinear manner.[4]

The STCA heat treatment of B/Al affects system behavior in two important ways. As is true of heat-treated aluminum, the grain structure is altered significantly, resulting in improved strength properties. More important to this study, the heat treatment significantly alters the stiffness properties of the 6061 aluminum matrix. In the condition F material, the residual thermal strains in the aluminum are very large, well beyond the yield point in tension, because of the fabrication cooldown phase. The material is diffusion bonded at a maximum fabrication temperature of 980° F and is cooled slowly in the furnace to room temperature, 70° F. The large variation in coefficients of thermal expansion for the boron fiber and aluminum matrix results in these large residual thermal strains. The aluminum in the STCA material, on the other hand, is very close to being free of residual stresses, because of the cryogenic quench to −320° F and subsequent warming to room temperature. Although the longitudinal tension stress-strain response of a unidirectional condition F laminate is fairly linear to failure, the aluminum matrix plastically deforms in tension from the very outset of load application. In comparison, the aluminum in a virgin STCA laminate responds elastically over most of the stress-strain curve, both in tension and compression.

Typical stress-strain data for 0, 90, $0/\pm 45$, and ± 45 condition F, and STCA B/Al are compared to typical data for G/E in Fig. 5. Note that the stress-strain response of condition F B/Al is much more nonlinear than that of STCA B/Al, and that B/Al, in general responds in a more nonlinear fashion than does G/E. The early mode I fracture work[1] with

Received May 13, 1975; presented as Paper 75-786 at the AIAA/ASME/SAE 16th Structures, Stuctural Dynamics, and Materials Conference, Denver Colo., May 27-29, 1975; revision received Jan. 12, 1977.

Index categories: Structural Composite Materials (including Coatings); Materials, Properties of; Structural Static Analysis.

*Senior Structures Engineer. Member AIAA.

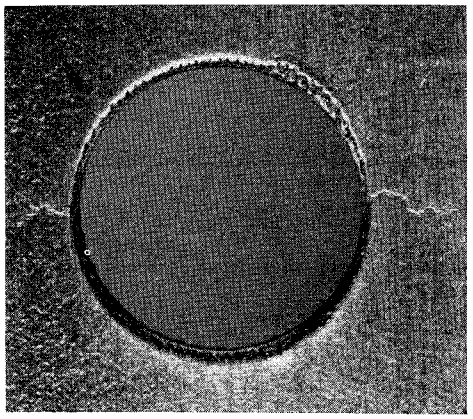

Fig. 1a Slow crack growth in (0/±45) B/Al; observed crack in tensile specimen.

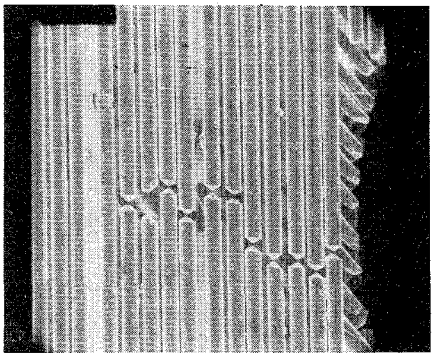

Fig. 1b Slow crack growth in (0/±45) B/Al; closeup of crack in 0° fibers in tensile specimen.

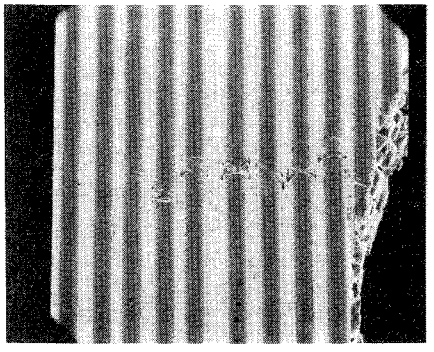

Fig. 1c Slow crack growth in (0/±45) B/Al; closeup of crack in bolt-bearing specimen.

resin-matrix composites partially succeeded in applying LEFM, originally developed for an elastic homogeneous isotropic material system, to an elastic, heterogeneous, anistropic material that consists of very stiff elastic fibers embedded in a fairly nonlinear, relatively low-stiffness resin matrix. The work reported here defines the degree to which LEFM also can be applied to a heterogeneous anisotropic material system consisting of the same very stiff elastic fibers, embedded now in either an elastic or basically plastic aluminum matrix (STCA or condition F material, respectively).

Experimental Progam

Materials

The material system investigated was 5.6-mil boron filaments embedded in a 6061 aluminum matrix. Consolidated 0° ±45°, and 0/±45° sheets of this material were purchases from Amercom. The fabrication procedure for this material involves a diffusion bonding process that occurs at

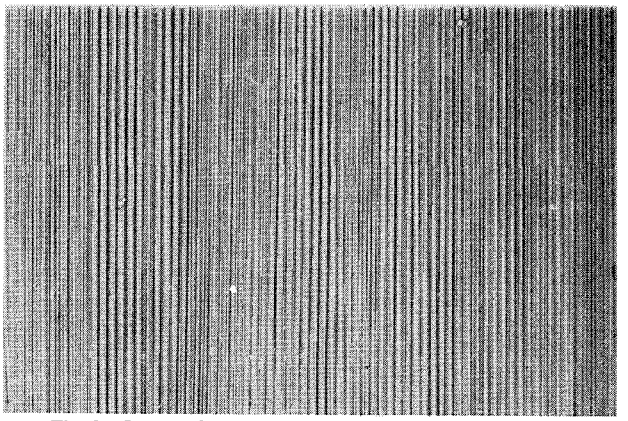

Fig. 2 Impact damage on an 0_4 condition F B/Al tube.

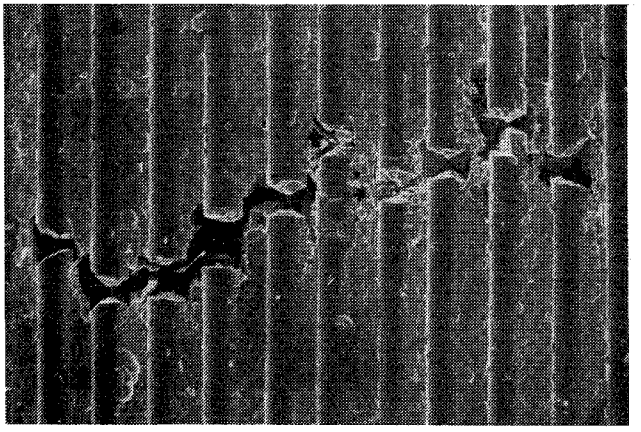

Fig. 3 Series of broken fibers in a unidirectional tension coupon.

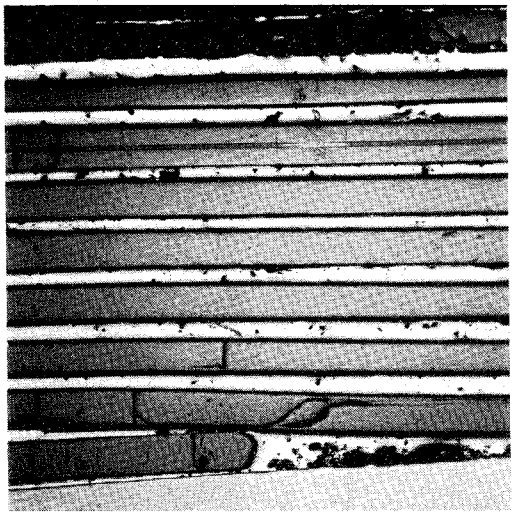

Fig. 4 Termination of a B/Al ply in a joint.

approximately 980° F and 10,000-psi pressure. To insure an adequate diffusion bond between the aluminum and boron fibers, the material is held at 980° F for approximately 5 min. and then is slowly cooled to room temperature. The material at this point is referred to as condition F or as-received. Because of the relative stiffness of the boron fiber and aluminum matrix, the condition F material contains an aluminum matrix that is at the yield point in tension, resulting from the cooldown residual thermal strains induced in fabrication. To relieve these thermal strains, it is sometimes necessary to heat treat the B/Al before using it in a particular application. Although two different heat treatment processes currently are being used for B/Al, the present study is con-

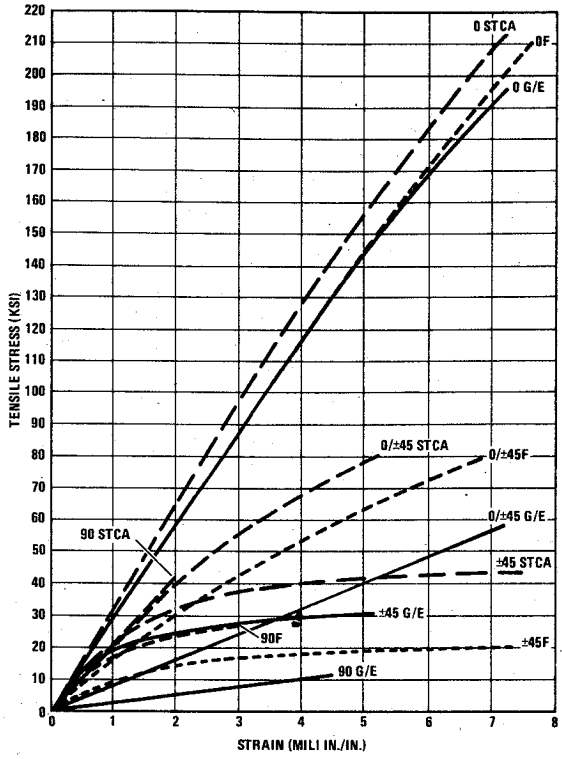

Fig. 5 Comparison of B/Al and G/E laminate stress-strain data.

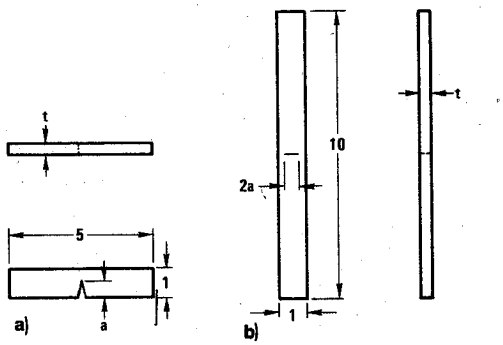

Fig. 6 Test specimen dimensions. All dimensions in inches. a) three-point bend specimen; b) center-notched specimen.

fined to the more popular STCA heat treatment. The as-received material first is subjected to 970° F for 30 min. The plate then is withdrawn from the furnace and immediately subjected to a water quench. For the STCA heat treat, the material then is soaked in liquid nitrogen (-320° F) for 5 min. before aging. The aging process takes place at 350° F for a minimum of 8 hrs, after which the plate is cooled slowly to room temperature inside the aging furnace. The STCA process was used at Convair in heat treating 75% of the fracture specimens.

All the incoming B/Al was subjected to three different quality-control tests upon receipt. The first test involved the determination of the fiber volume percent for each of the plates. Samples of each plate were weighed, the aluminum then was leached away using NaOH, and the fibers were dried and reweighed to determine the fiber weight percent. Knowing the fiber weight percent and the densities of the fiber and aluminum, the fiber volume percent for each plate was determined. The results are listed in Table 1.

The specification called out in the material purchase order required that the fiber volume percents of each plate be in the range of 45.0±2.5%. As can be seen, these plates were within the specification limits. The second quality-control test involved fabricating small tensile coupons from each plate and

Table 1 B/Al fiber volume percents

Orientation	Fiber Volume %
0_{10}	47.2
0_{20}	46.7
0_{40}	47.5
$(\pm 45)_{3s}$	46.9
$(0/\pm 45)_{2s}$	46.8
$(\pm 45)_{9s}$	–
$(0/\pm 45)_{6s}$	–
$(0/\pm 45)_{s}$	43.7

testing each to failure tension. The third test involved taking boron fibers that had been leached from the plates and performing fiber bend tests to insure a minimum strength requirement for this lot of boron fibers. The results of the static tests and fiber bend tests proved sufficient to accept the delivered materials.

Procedures

An electrical discharge machine (EDM) was used to notch all the B/Al fracture specimens. Originally, a 15-mil-thick carbon electrode was used to notch the B/Al specimens. This method proved to be satisfactory for those specimens which were 10 to 12 plies thick. For thicker specimens, however, the carbon electrode burned through the specimens at a relatively slow rate, causing the entrance notch width to be much larger than the exit notch width. The resulting entrance notch widths did not satisfy the tolerance requirement set for these specimens. To enable notching of the thicker specimens, a copper electrode, again approximately 15-mil-thick, was used to discharge the slots, electrically. This new electrode material proved sufficient to maintain the width tolerance requirements. For the thinner specimens, the machining operation required approximately 6 min. of cutting time. For the thicker specimens, approximately 15 min. were required.

All tests were run at room temperature. For the thinner specimens, where stability has in the past proven to be a problem, Teflon-coated aluminum side support plates were used for lateral support. Specimens 20 plies thick and greater did not require the side support plates. The center-notch specimens were tested in tension using standard wedge action jaws. Because of the severity of the center notches, it was not necessary to use doublers for load introduction. The instrumentation used for both the center-notch and three-point bend specimens consisted of load vs head displacement (P vs δ) and load vs crack opening displacement (P vs COD). The crack opening displacement gages in both cases were mounted using removable clips.

Tests

A description of the 59 B/Al fracture specimens tested during the program is presented in Table 2. Standard three-point bend (TPB) and center-notched specimens (CN) were used for static fracture tests to failure. The details of the specimen dimensions are shown in Fig. 6. Three different unidirectional laminate thicknesses (10, 20, and 40 plies) and two cross-plied laminate thicknesses (12 and 36 plies) were run to evaluate the effect of thickness on mode I fracture toughness, K_Q. As mentioned previously, both conditon F (as received) and heat treated (STCA) B/Al were investigated. To evaluate the effects of specimen geometry on material fracture toughness, two different fracture specimens were selected: again, the three-point bend and center-notched specimens. Although it was not economically feasible to evaluate the effects of stacking sequence on laminate fracture

Table 2 Description of B/Al fracture tests

Test Specimen	No.	CL (in.)	L (in.)	W (in.)	Test Specimen	No.	CL (in.)	L (in.)	W (in.)
0_{10} TPB-H	3	0.35	5	1	0_{10} CN-F	3	0.45	10	1
0_{10} TPB-H	3	0.45	5	1	0_{20} CN-H	3	0.45	10	1
0_{10} TPB-F	3	0.45	5	1	0_{40} CN-H	3	0.45	10	1
0_{10} TPB-H[a]	3	0.45	5	1	$(\pm 45)_{3s}$ TPB-H	3	0.45	5	1
0_{10} TPB-H	3	0.55	5	1	$(\pm 45)_{3s}$ TPB-F	1	0.45	5	1
0_{10} TPB-F	3	0.55	5	1	$(\pm 45)_{9s}$ TPB-H	3	0.45	5	1
0_{20} TPB-H	3	0.45	5	1	$(\pm 45)_{3s}$ CN-H	3	0.45	10	1
0_{20} TPB-F	1	0.45	5	1	$(0/\pm 45)_{2s}$ TPB-H	3	0.45	5	1
0_{40} TPB-H	3	0.45	5	1	$(0/\pm 45)_{2s}$ TPB-F	1	0.45	5	1
0_{40} TPB-F	3	0.45	5	1	$(0/\pm 45)_{6s}$ TPB-H	2	0.45	5	1
0_{10} CN-H	3	0.45	10	1	$(0/\pm 45)_{2s}$ CN-H	3	0.45	10	1

[a]Specimens heat treated following EDM notching
TPB = three-point bend
CN = center notch
F = Condition F or "as received"
H = heat treated to STCA condition (solution treated, cryogenically quenched & aged)
CL = total notch length
L, W = specimen length, width (inches)

toughness, this variable also must be considered. For the STCA material, the sequence of EDM notching and heat treating was varied to determine the effect of this sequence of operations. Since the EDM operation involves local heating of the specimen, possible annealing effects could occur at the crack tip, which would alter the apparent fracture toughness. It is believed that both sequences could represent physical conditions. In the case of notching after heat treatment, production drilling could result in a very similar annealing type process near a circular cutout. If an internal ply were terminated, or damaged boron filaments were present in the condition F material, a heat-treated part would exhibit a fracture toughness similar to that observed for those test specimens where heat treatment followed the EDM notching.

A majority of the specimens were tested for the case in which notching occurred after heat treatment, since it was believed that this would result in the lower fracture toughness values, which at least would be conservative.

Analytical Methods

In calculating mode I fracture toughness values from the experimental test data, two expressions derived for metals fracture testing were used. To reduce the three-point bend test data the expression given in Eq. (1) was used[5]

$$K_Q = (P_Q S/BW^{3/2})\, Y(a/W) \tag{1}$$

where

$$Y(a/W) = 2.9(a/W)^{1/2} - 4.6(a/W)^{3/2} + 21.8(a/W)^{5/2} - 37.6(a/W)^{7/2} + 38.7(a/W)^{9/2}$$

K_Q = candidate fracture toughness
P_Q = candidate fracture load
S = span
B = thickness
W = width
a = total crack length

It has been assumed that the isotropic correction term $Y(a/W)$ is applicable to this work. In analyzing the center-notch test data, Eq. (2), which was developed for isotropic materials,[6] was used

$$K_Q = (P_Q a^{1/2}/BW)\, Y(2a/W) \tag{2}$$

where

$$Y(2a/W) = 1.77[1\text{-}0.1\,(2a/W) + (2a/w)^2]$$

$2a$ = total crack length

Rather than testing each possible crossplied laminate combination to determine fracture toughness values, it would be advantageous to have a theoretical method to predict laminate fracture toughness values which used basic lamina fracture toughness data. Such a method has been proposed and successfully applied to G/E materials.[1] Assuming that colinear crack growth occurs uniformly through the thickness of a $0/\pm\alpha/90$ laminate, the proposed method theoretically can predict the fracture toughness of the laminate based on the fracture toughness values of the laminate's constituent plies, using a strain energy approach. The critical strain energy release rate for a $\pm\alpha$ laminate, G_Q^α, can be calculated from the fracture toughness of the $\pm\alpha$ laminate, K_Q^α using

$$G_Q^a = -\frac{(K_Q^a)^2}{2}\beta_{22}^\alpha \operatorname{Im}\left[\frac{\mu_1^a + \mu_2^a}{\mu_1^a \mu_2^a}\right] \tag{3}$$

where the μ^a's are functions only of the $\pm\alpha$ laminate's compliance matrix data $[\beta]$. The characteristic values, μ_1 and μ_2, are roots of the following fourth-order characteristic equation[7]

$$\beta_{11}\mu^4 - 2\beta_{16}\mu^3 + (2\beta_{12} + \beta_{66})\mu^2 - 2\beta_{26}\mu + \beta_{22} = 0 \tag{4}$$

To predict analytically the fracture toughness of a $0/\pm\alpha/90$ laminate from K_Q^0, K_Q^α, and K_Q^{90}, it is assumed that the strain energy released during crack growth in the laminate, G_Q^L, is equal to the thickness weighted average of the individual ply strain energy release rates calculated from Eq. (3). Mathematically

$$G_Q^L = \Sigma\, t_a G_Q^a / t_L \tag{5}$$

Having G^L and the μ^L values, K_Q^L can be calculated using

$$K_Q^L = \left[\frac{-2G_Q^L}{\beta_{22}^L \operatorname{Im}[(\mu_1^L + \mu_2^L)/\mu_1^L \mu_2^L]} \right]^{1/2} \quad (6)$$

Here β_{22}^L, μ_1^L, and μ_2^L represent material constants for the $0/\pm\alpha/90$ laminate.

Analytical predictions for the fracture toughness of $(0/\pm 45)$ boron/aluminum laminates using these equations are compared to the experimental results in the next section. When using this type of strain-energy-based prediction theory, it is important that all of the absorbed strain energy be used in propagating the mode I crack. As a result, care must be taken in any test program to observe and account for other possible energy absorption mechanisms, such as intralaminar shear failures or interlaminar delamination damage. The latter is typical of epoxy resin systems; the former has been observed for B/Al in this study.

As has already been observed, the assumption of through-the-thickness colinear crack growth probably is not valid in a number of cases. The crack that propagated radially from the circular hole in the $(0/\pm 45)$s laminate (Fig. 1) initially grew through only the 0° plies and not the ±45° plies. Although such a phenomenon does occur in a tensile coupon containing a circular cutout, the through-the-thickness crack growth assumption may be valid for $(0/\pm 45)$ fracture specimens since the 45° plies immediately adjacent to the crack in Fig. 1 are not continuous. As a result, the ±45° plies do not allow a crack to propagate through them until the first continuous fiber is reached. Care must be taken to identify the governing failure mechanism before applying a fracture-based strength model to any static test article.

Results

The data reduction scheme used in calculating fracture toughness values is slightly different from that proposed for metals fracture tests.[5] As discussed previously, the nonlinearity of the aluminum matrix can affect significantly the stress-strain response of both unidirectional and crossplied B/Al tensile coupons. In general, the load vs head displacement and load vs crack opening displacement (*COD*) response for both the three-point bend and center-notched specimens were quite nonlinear. Typical *P* vs *COD* curves are presented in Fig. 7. Rather than severely penalizing our calculations of fracture toughness by using an initial slope reduction of 5% as is recommended in Ref. 5, p., 437, the maximum load achieved during the test P_{max}, was used as the candidate fracture load P_Q. The major justification for using P_{max} as P_Q is that the predicted fracture toughness values using such an approach should represent closely the behavior that will be exhibited in most structural applications. In general, no definite pop-in load could be identified for these various fracture tests.

A summary of the B/Al fracture toughness data generated under this program is presented in Table 3. To investigate the effect of crack length on fracture toughness, a number of the initial 10-ply unidirectional tests were run with varying crack lengths (0.35, 0.45, and 0.55 in.). The fracture toughness data for these three-point bend tests are summarized in Fig. 8. The experimental correlation between K_Q and crack length is reasonably good except for the 0.55 in. crack in the STCA material. It is believed that this discrepancy can be attributed, in part, to misalignment of the applied load with the crack plane in the three-point bend specimens, which had a total crack length of 0.55 in. It became apparent from these test

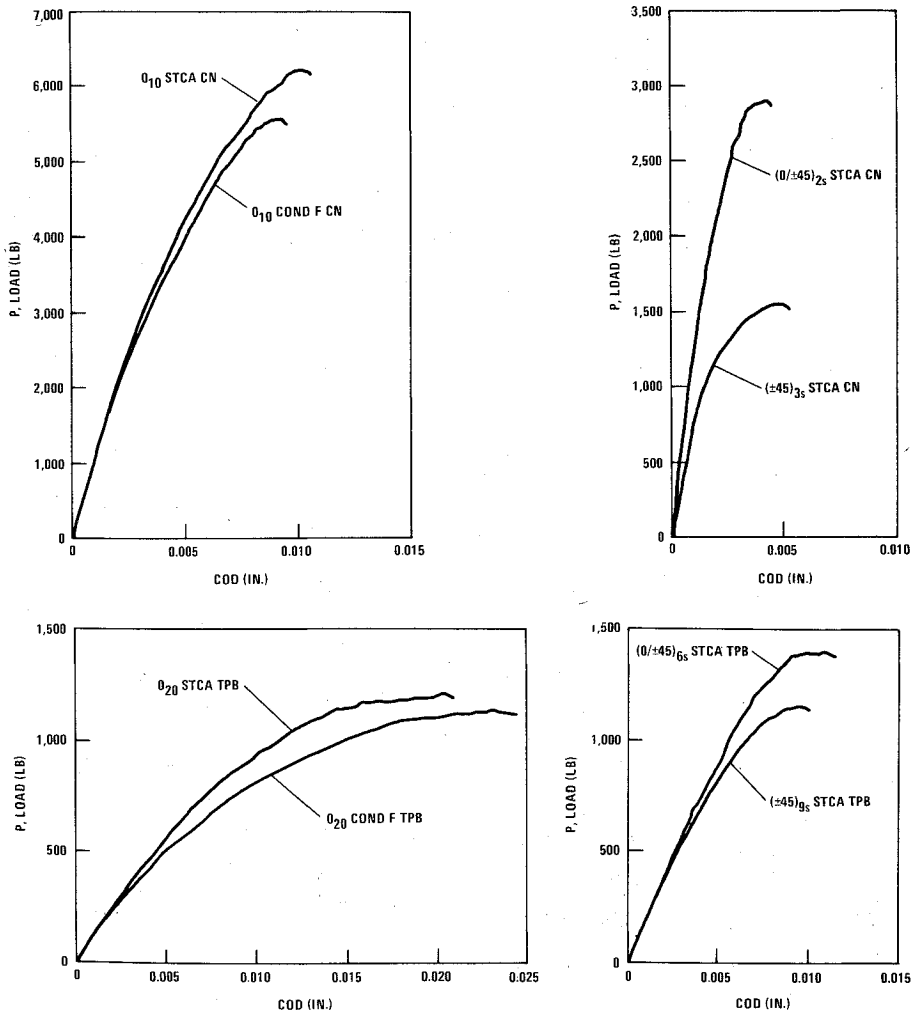

Fig. 7 Typical *P* vs *COD* curves.

Table 3 Summary of B/Al fracture toughness data

Test Specimen		CL	K_Q			avg K_Q	avg σ_{net}/F_{tu}	avg σ^a_{max}/F_{tu}
0_{10}	TPB-H	0.35	85.0	86.5	78.0	83.2		0.81
0_{10}	TPB-H	0.45	84.0	84.0	85.5	84.5		0.87
0_{10}	TPB-F	0.45	70.6	69.6	68.6	69.6		0.68
0_{10}	TPB-H[a]	0.45	95.1	96.5	111.4	101.0		1.03
0_{10}	TPB-H	0.55	77.7	75.7	80.4	77.9		0.86
0_{10}	TPB-F	0.55	66.2	70.0	72.4	69.5		0.75
0_{20}	TPB-H	0.45	76.4	63.2	76.7	72.1		0.75
0_{20}	TPB-F	0.45	68.8	—	—	68.8		0.69
0_{40}	TPB-H	0.45	81.5	78.0	78.5	79.3		0.83
0_{40}	TPB-F	0.45	68.3	68.3	68.0	68.2		0.68
0_{10}	CN-H	0.45	85.5	87.4	82.5	85.1	0.76	
0_{10}	CN-F	0.45	74.7	77.9	70.8	74.5	0.64	
0_{20}	CN-H	0.45	83.6	80.6	76.7	80.3	0.72	
0_{40}	CN-H	0.45	88.0	88.6	88.1	88.2	0.75	
$(\pm45)_{3s}$	TPB-H	0.45	32.1	30.9	30.3	31.1		1.10
$(\pm45)_{3s}$	TPB-F	0.45	29.3	—	—	29.3		1.35
$(\pm45)_{9s}$	TPB-H	0.45	37.3	38.5	39.0	38.3		1.34
$(\pm45)_{3s}$	CN-H	0.45	17.0	17.6	18.1	17.6	0.84	
$(0/\pm45)_{2s}$	TPB-H	0.45	43.5	48.0	42.5	44.7		1.15
$(0/\pm45)_{2s}$	TPB-F	0.45	40.6	—	—	40.6		1.12
$(0/\pm45)_{6s}$	TPB-H	0.45	45.4	46.5	—	46.0		1.18
$(0/\pm45)_{2s}$	CN-H	0.45	32.7	33.4	33.9	33.3	0.72	

[a] $\sigma_{max} = Mc/I$

results that extreme care must be taken to insure proper alignment of the applied load with the crack axis. Where misalignment was the greatest, cracks initially grew in a direction parallel to the fibers until the crack tip reached a point directly below the load application point, at which time the crack began to grow across fibers as it should have originally.

The data presented in Table 3, which describes the effect of thickness on fracture toughness, have been plotted and are presented in Fig. 9. A thickness effect is not apparent. Since the fracture toughness data neither consistently increases nor decreases, it appears that the effect of thickness is negligible and that the variations exhibited in a fracture toughness may be due merely to experimental error. As a result, horizontal lines have been drawn through the average fracture toughness value for each of the four plots presented.

In comparing the predicted fracture toughness values for the STCA three-point bend and center-notch specimens, the data seems to be in agreement for the 0° tests, but the ±45 and 0/±45° tests show a significant decrease in fracture toughness for the center-notch specimens. This disagreement is due in part to our using the isotropic finite size correction factors in reducing these orthotropic results. A second possible explanation involves the validity of the various fracture tests. Also presented in Table 3 are two stress ratios, one

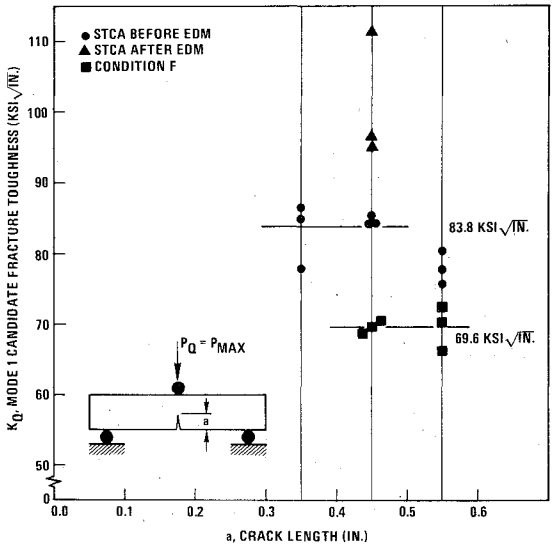

Fig. 8 0_{10}B/Al three-point bend fracture results, K_Q vs α.

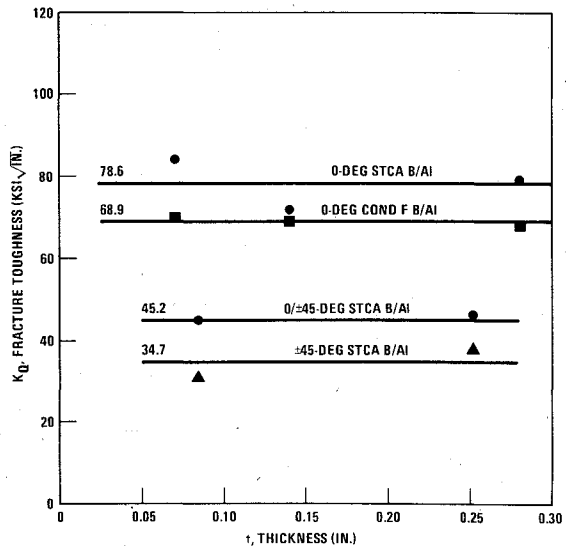

Fig. 9 K_Q vs thickness for three-point bend tests.

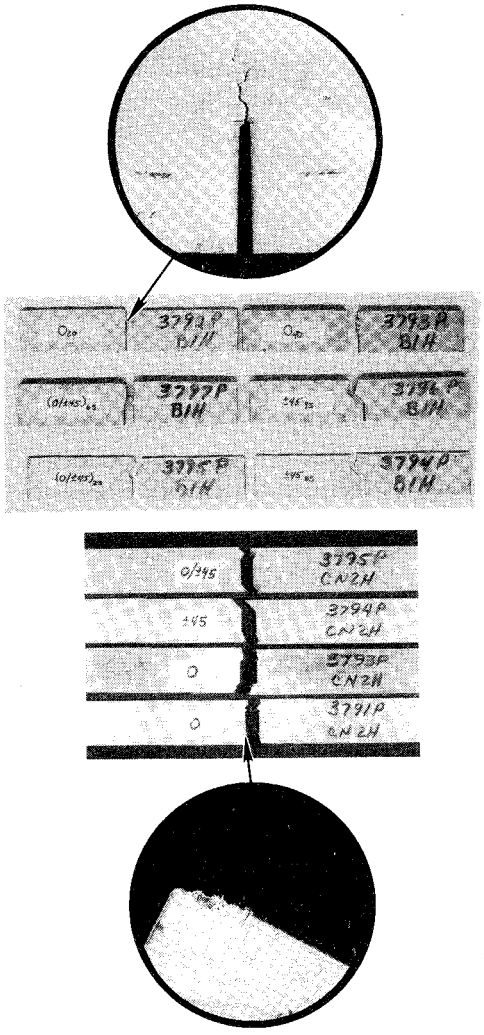

Fig. 10 Fracture surface details.

for the center-notch test and one for the three-point bend tests, which provide some indication of the true notch sensitivity of the various test specimens. For a center-notch test to be considered a valid test, it is proposed[8] that $\sigma_{net}/F_{tu} \leq 0.6$. As can be seen from Table 3, all of the center-notch results in the program fall between 0.64 and 0.84, which casts some doubt on the validity of these results. In the case of the three-point bend tests, it is proposed that the ratio of $\sigma_{max}/F_{tu} \leq 1.0$ for a valid test.[8] The table shows that only the 0° three-point tests satisfy this requirement. For the crossplied three-point bend specimens, $1.10 \leq \sigma_{max}/F_{tu} \leq 1.35$.

Photographs showing the details of the fracture process for typical 0°, ±45°, and 0/±45° fracture specimens are shown in Fig. 10. In the 0° TPB and CN specimens, localized shear failures are observed at the crack tip (Fig. 10.). Since these cracks represent another energy sink, their effect must be considered when discussing fracture analyses of UD material. Similar damage was not exhibited by the crossplied specimens.

Prediction of Laminate Fracture Toughness

The strain energy-based theory previously discussed was applied to the prediction of K_Q for condition F and STCA 0/±45 boron-aluminum laminates. Since the effect of thickness on fracture toughness has been shown to be small, if not negligible, the theoretical predictions were based on the average fracture toughness values for the various thickness specimens tested , as summarized in Table 3. To perform these calculations, the characteristic constants μ_1 and μ_2 and β_{22} were required for the three various laminate orientations

Table 4 Material constant data

Material Constant	Condition F B/Al	STCA B/Al
Lamina Properties		
E_{11} (x 10^6 psi)	30.5	33.2
E_{22} (x 10^6 psi)	22.4	22.7
G_{12} (x 10^6 psi)	8.65	8.91
ν_{12}	0.29	0.26
0-Degree Laminate		
μ_1	0.0 +0.75765 i	0.0 +0.74216 i
μ_2	0.0 + 1.54012 i	0.0 +1.62953 i
β_{22}	4.46429 x 10^{-8}	4.40529 x 10^{-8}
±45-Degree Laminate		
μ_1	0.35353 +0.93542 i	0.39056 +0.92058 i
μ_2	-0.35353+0.93542 i	-0.39056+0.92058 i
β_{22}	4.31407 x 10^{-8}	4.21459 x 10^{-8}
0/±45-Degree Laminate		
μ_1	0.21301 +1.00538 i	0.23853 +1.00672 i
μ_2	-0.21301+1.00538 i	-0.23853+1.00672 i
β_{22}	4.34241 x 10^{-8}	4.74717 x 10^{-8}

Table 5 Summary of K_Q data and predictive capability

Fracture Toughness	Plies	TPB-H	TPB-F	CN-H	CN-F
$K_Q(0)$	10	84.5	69.6	85.1	74.5
	20	72.1	68.8	80.3	—
	40	79.3	68.2	88.2	—
		78.6	68.9	84.5	
$K_Q(\pm 45)$	12	31.1	29.3	17.6	—
	36	38.3	—	—	—
		34.7			
$K_Q(0/\pm 45)$	12	44.7	40.6	33.3	—
	36	46.0	—	—	—
		45.2			
Pred K_Q $(0/\pm 45)$		54.8	47.3	52.7	—
Error		21.2%	16.5%	58.3%	—

TPB = three-point bend
CN = center notch
H = heat-treated (STCA)
F = Condition F

(i.e., 0, ±45, and 0/±45). A summary of the material constant data used in these calculations is presented in Table 4. The results of the analyses are summarized at the bottom of Table 5. In each case the predicted value of K_Q (0/±45) was high or unconservative by from 16.5% to 58.3%. It is believed that the major contributing factor to this overprediction of fracture toughness was the artifically high fracture toughness values experimentally determined for the 0° specimens. Since these unidirectional specimens absorbed some energy in a shear mode, the calculated experimental fracture toughenss values are high. As a result, the use of such an energy based criteria is not feasible without accounting for this additional energy sink in the calculations. Further work needs to be performed in this area. In the crossplied laminate, the shear failures apparently were suppressed by the adjacent

crossplies. Perhaps these effects can be accounted for using some pseudo-plastic zone, similar to that currently used in analyzing metal fracture tests.

Conclusion and Recommendations

Although the limited data presented in this study have revealed a number of problems involved in applying fracture mechanics to 5.6-mil boron/6061 aluminum, it is felt that fracture mechanics does represent a potentially valuable data reduction scheme for analyzing the types of structural problems discussed in the "Introduction."

This study has begun to define those conditions under which LEFM is applicable to boron/aluminum. The test data reported indicates that the effects of specimen thickness and crack length on fracture toughness are negligible. Fracture toughness data have been presented for 0, ±45, and 0/±45 laminates, in both the condition F and STCA material. A strain-energy-based technique of predicting the fracture toughness value of a crossplied laminate from the fracture toughness values of its constituent plies was investigated. The method was inadequate, since the development of intrafiber shear cracks at the notch tip resulted in artificially high 0° fracture toughness values. The predictions for the fracture toughness of the 0/±45 laminates were, in turn, high by 16.5 to 58.3%.

Two unforeseen results emerged from the test program. Specimens that were notched before heat treat attained an increased fracture toughness of about 20% over those that were heat treated before notching, even though the former did exhibit some warpage near the crack tip. The second result involves the relatively nonlinear behavior of these fracture specimens during loading. Both load vs *COD* and load vs head displacement curves were fairly nonlinear. These two experimental results warrant further investigation.

Several related topics not investigated in this work should be considered to evaluate further the usefulness and applicability of fracture mechanics principles to boron/aluminum:

1) Study the effect of part-through cracks vs through cracks. Plane strain effects may inhibit shear failures in unidirectional B/Al and result in lower fracture toughness values.

2) Run tests to evaluate the effect of stacking sequence, geometry variations, and environment on fracture toughness.

3) Perform impact tests to evaluate the applicability of using fracture mechanics to predict residual strengths of damaged B/Al structures.

4) Investigate the effect of internal ply terminations using a fracture mechanics model.

5) Test nearly unidirectional laminates (e.g., ±5 to ±10) to determine whether a small crossply could retard intrafiber shear failures successfully.

References

[1]Konish, H. J., Jr., "A Study of Fracture Phenomena in Fiber Composite Laminates," Air Force Materials Laboratory, Wright-Patterson AFB, Ohio, AFML-TR-73-145, Vol. III, Sept. 1973.

[2]Waddoups, M. E., Eisenmann, J. R., and Kaminski, B. E., "Macroscopic Fracture Mechanics of Advanced Composite Materials," *Journal of Composite Materials*, Vol. 5, 1971, p. 446.

[3]Ashton, J. E., Halpin, J. C., and Petit, P. H., *Primer on Composite Materials: Analysis*, Technomic Publishing Co., 1969.

[4]Waszczak, J. P. et al., "Structural Analysis Methods for Advanced Composites," General Dynamics Convair Division, San Diego, Calif., CASD-ERR-73-029, Dec. 1973.

[5]"Standard Method of Test for Plane-Strain Fracture Toughness of Metallic Materials," E399-74, *1974 Annual Book of ASTM Standards*, Part 10, p. 438.

[6]Brown, W. F., Jr., and Srawley, J. E., "Plane-Strain Crack Toughness Testing of High Strength Metallic Materials," ASTM STP 410, 1966, p. 11.

[7]Lekhnitskii, S. G., *Theory of Elasticity of an Anisotropic Elastic Body*, Holden-Day, 1963.

[8]Osias, J. O, and Cruse, T. A., "Exploratory Development on Fracture Mechanics of Composite Material," Air Force Materials Laboratory, Wright-Patterson, AFB, AFML-TR-74-111, April 1974.